ABSTRACT

Title of Thesis:	MULTI-FUNCTIONAL NANOSTRUCTURED FILMS FROM CELLULOSE NANOFIBERS
	Soo-Hwan Jang, Master of Science, 2017
Thesis Directed By:	Professor Liangbing Hu, Department of Materials Science and Engineering

Cellulose nanofibrils (CNF) are one of most popular materials in nanotechnologies due to its favorable properties, such as biodegradability and high mechanical performance. However, their nano-/microscopric structure is not fully understood. In this thesis, we studied the structural features of CNF by using atomic force microscopy (AFM) and scanning electron microscopy (SEM), and then assessed the dimensions of single fibers from different wood species. We studied the dependence of cellulose nanopaper strength and toughness on the size of cellulose fibers using dynamic mechanical analysis (DMA). Interestingly, we found that both the strength and toughness increased as the fiber aspect ratio increased. Additionally, stability tests of carbon nanotubes and cellulose nanofibrils (CNT-CNF) solution were conducted by rheological measurement. The solution showed high stability and no visible precipitation. Based on these properties, we fabricated functionalized

nanostructured films from CNF and observed promising results from the novel materials.

MULTI-FUNCTIONAL NANOSTRUCTURED FILMS FROM CELLULOSE NANOFIBERS

by

Soo-Hwan Jang

Thesis submitted to the Faculty of the Graduate School of the
University of Maryland, College Park, in partial fulfillment
of the requirements for the degree of
Master of Science
2017

Advisory Committee:
Professor Liangbing Hu, Chair
Professor Teng Li
Professor Yifei Mo

Dedication

To the memory of my grandfather

Hyunjoo Lee

1927 - 2017

For his unconditional love and endless prayer to me

Acknowledgements

First and foremost, I would like to express my sincere gratitude to my advisor Professor Liangbing Hu for his continuous support of my study and research. His guidance helped me during the time I spent researching and writing my thesis. I will always remember and appreciate his mentorship and enthusiasm which he showed to me as my advisor.

Besides my advisor, I would like to say a big thank the rest of my thesis committee: Professor Teng Li and Professor Yifei Mo for their sharp-witted comments and great encouragement.

My sincere thanks also goes to all my graduate course professors of University of Maryland for their valuable teaching to make me wide scientific knowledge.

Also, I thank the constant assistance and cooperation of the Bing Research Group members, especially Wei Luo, Yubing Zhu, and Yilin Wang. I also thank Steven Lacey, Jaiqi Dai, and all the other group members for offering advice and supporting me throughout graduate school.

Last but not least, I would like to express the incredible support from my family throughout graduate school and all my life. Without their love, I could not have gotten to this point. I would also like to express my warmest love to my grandfather who passed away during my study.

I would like to thank God for everything.

Table of Contents

List of Figures

List of Abbreviations

AFM- Atomic force microscopy

AgNW - Silver nanowires

BKP - Bleached kraft pulp

CMC - Cellulose microcrystal

CNC - Cellulose nanocrystal

CNF - Cellulose nanofibrils

CTE - Coefficient of thermal expansion

DMA - Dynamic mechanical analysis

MFC - Microfibrillar cellulose

NaBr - Sodium bromide

NaClO - Sodium hypochlorite

NaOH - Sodium hydroxide

NFC - Nanofibrillated cellulose

NP - Nanopapers

PC - Polycarbonate

PEN - Polyethylene naphthalate

PET - Polyethylene terephthalate

RMS - Root mean square

SEM - Scanning electron microscopy

TAPPI - Technical Association of the Pulp and Paper Industry

TEMPO - 2,2,6,6-tetramethylpoperidine-1-oxyl

TOF - TEMPO-oxidized fibers

Chapter 1: Introduction

1.1 Motivation for development of a new type of flexible substrates

Flexible plastic substrates are ubiquitous in electronic devices because of their excellent mechanical properties, roll-to-roll processing capability, low cost and being lightweight. Plastic substrates already host high-performing devices such as organic solar cells, light-emitting diodes, transistors, and circuits [1]. Typical flexible substrates are polyethylene terephthalate (PET), polyethylene naphthalate (PEN), and polycarbonate (PC). Although plastic substrates have certainly achieved success in a variety of devices, they carry several disadvantages that drive a need to replace them in certain applications. For example, plastic substrates possess a low coefficient of thermal expansion (CTE) and processing temperature, and in some cases are not renewable, based on petro chemistry [2]. Plastic substrates are also inferior to paper substrates for roll-to-roll printing. Extra additives are needed to enable ink to be printed on a plastic substrate. Paper has attracted much attention as an emerging substrate for flexible electronics and optoelectronics [3].

1.1.1 Traditional paper

Since the invention of papermaking around AD 105, paper has been one of the most widely used materials in everyday life [1]. Paper is used for a variety of purposes, such as writing, drawing, packing, etc. Usually, regular paper is made from

cellulose fibers having a diameter of 10-50 μm (Figure 1). Those cellulose fibers consist of a large number of microfibrils having a diameter of < 1 μm. The microfibrils themselves are made of nanofibrils, having a diameter of < 0.1 μm (Figure 2).

Recently, paper has attracted a lot of attention for the possibility of its application in electronic devices due to its cost-effectiveness, ease of mass production, flexibility, natural abundance and environmental friendliness. The price of paper (~ 10 cent/m^2) is much lower than that of conventional plastics, such as polyethylene terephthalate (~ 2 dollar/m^2) [4]. Further, its long history as a high-speed roll-to-roll process increases the competitiveness. All of these properties, including flexibility, make regular paper one of the strongest candidates for replacing conventional plastic substrates for electronics. However, surface roughness, opaqueness, and the porous structure of cellulose paper have delayed its incorporation into industrial applications for optoelectronics (Figure 1).

Figure 1. A bundle of regular paper (left hand) and a SEM image of surface of regular paper (right hand).

1.1.2 Nanopaper

To overcome limitations of traditional paper, many researchers are making new types of paper with reduced surface roughness and/or increasing transparency [1]. To overcome surface roughness, paper based on nanofibrils are being invented, as they provide a smoother film than regular paper. Paper made of nanofibers are called nanopaper (NP). As shown in Figure 2, a paper becomes more clear and has a lower surface roughness than a traditional paper. Nanofibrils have extremely large specific surface areas, the properties of which are sometimes significantly different from those of the bulk materials; therefore, the research and development of nanofibers have been extensively promoted by both academia and industry in the nanotechnology field.

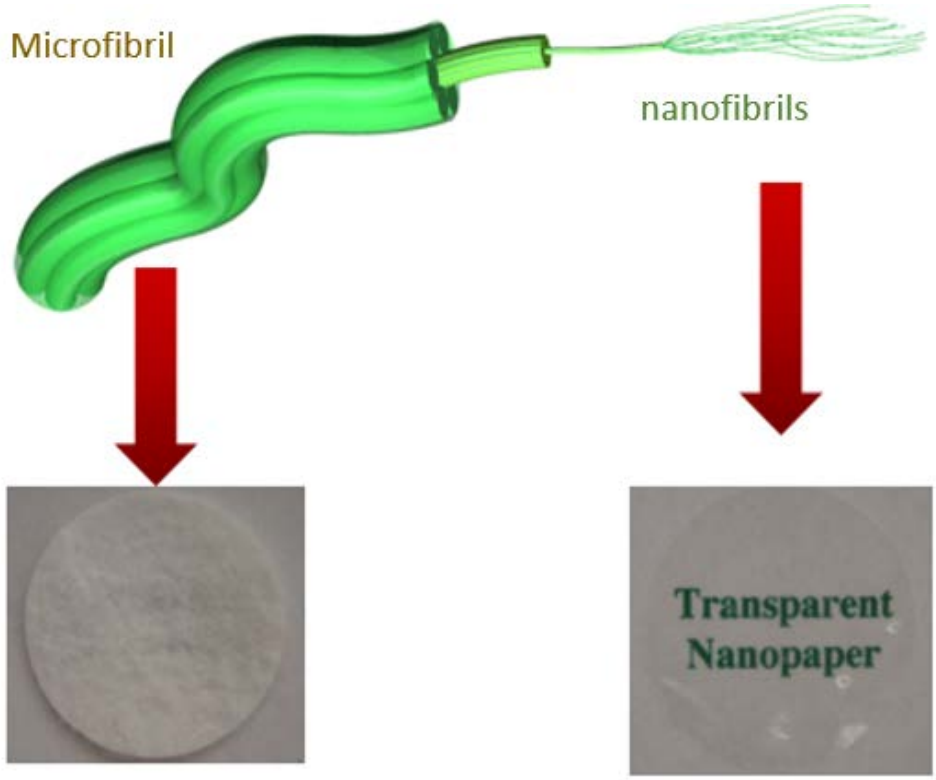

Figure 2. A Traditional paper and a nanopaper (NP).

1.2 Background

Wood is a biodegradable biopolymer and consists mainly of three chemical components: cellulose, hemicelluloses, and lignin [1]. Several published articles have presented detailed findings pertaining to these wood components [1,3,4]. The hierarchical structure of wood is presented in Figure 3, which shows both the macroscopic and microscopic structure of wood [1].

Hemicellulose has a random, amorphous polymer with little strength and crosslinks with elementary fibrils due to its structure. Lignin, which is also an amorphous polymer, acts as glue by associating with hemicellulose closely in wood [1]. Cellulose, which is composed of crystalline and amorphous regions, is usually found in a form of mixture with hemicellulose and lignin. Thus, removal of hemicellulose and lignin is an important part in order to get cellulose nanofibrils. Among processes for delignification like the mechanical process, the acidic sulfite process, and so on, the kraft process is most commonly used.

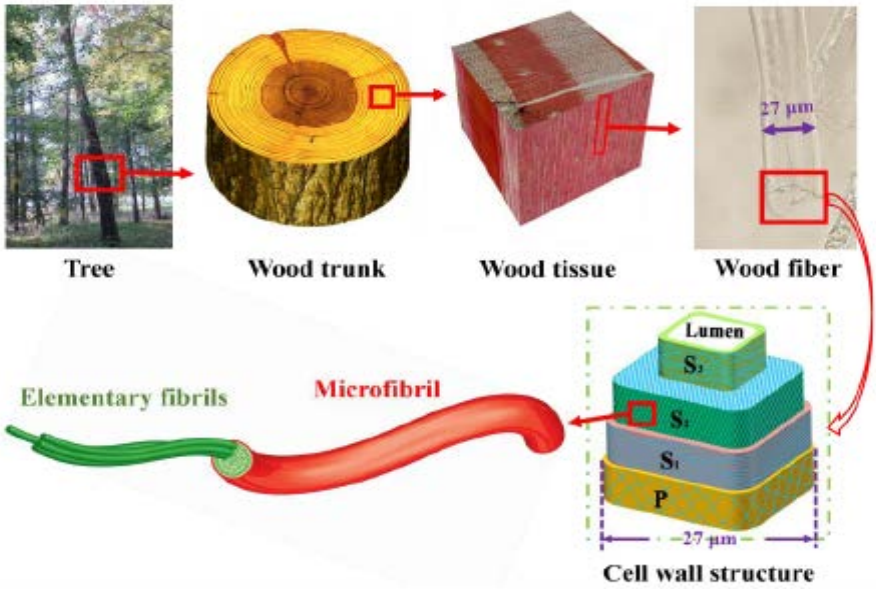

Figure 3. Schematic to show the hierarchical structure of wood fibers.

1.3 Kraft process and kraft pulp

The kraft process, also known as kraft pulping, is a process for conversion of wood into wood pulp, which consists of almost pure cellulose fibers, the main component of paper. The kraft process entails treatment of wood chips with a hot mixture of water, sodium hydroxide, and sodium sulfide that breaks the bonds that link lignin, hemicellulose, and cellulose. The technology entails several steps, both mechanical and chemical. It is the dominant method for producing paper. In some situations, the process has been controversial because kraft plants can release smelly products and in some situations produce substantial liquid wastes [5].

Pulp produced by the kraft process is stronger than that made by other pulping processes. The acidic sulfite processes degrade cellulose more than the kraft process, which leads to weaker fibers [5, 6]. Kraft pulping removes most of the lignin present originally in the wood whereas mechanical pulping processes leave most of the lignin in the fibers [6]. The hydrophobic nature of lignin interferes with the formation of the hydrogen bonds between celluloses needed for the strength of paper (strength refers to tensile strength and resistance to tearing) [6]. Kraft pulp is darker than other wood pulps, but it can be bleached to make very white pulp. Fully bleached kraft pulp is used to make high-quality paper, where strength, whiteness and resistance to yellowing are important. We used bleached kraft pulp (BKP) for fabricating CNF, also known as nanofibrillated cellulose (NFC). The kraft process can use a wider range of fiber sources than most other pulping processes. All types of wood, including very resinous types like southern pine [7], Eucalyptus [8] and non-wood species like sugarcane (or bagasse) [9] can be used in the kraft process.

1.4 Outline of this thesis

This thesis mainly focuses on CNF and its characteristics. The main objectives of the thesis are as follows:

- To study the process of producing CNF from bleached kraft pulps (BKP)
- To study the dimension of single fibers and physical characteristics of CNF film and its composites
- To study CNF to make flexible films
- To study the possibility of utilizing NFC with other materials such as silver nanowires (AgNW) for functionalized film applications
- To study the use of CNF as a surfactant and a paper strength additive in composite films.

Chapter 2 shows the process of production of CNF by chemical pretreatment with the mechanical process.

Chapter 3 focuses on the dimensions of CNF from various wood sources and physical characteristics of nanopapers.

Chapter 4 describes the functionalized nanopapers to introduce conductivity for optoelectronics and the potential of CNF as a surfactant.

Finally, chapter 5 summarizes our findings and provides an outlook for future work.

Chapter 2: Nanocellulose and its fabrication: Materials and methods

2.1 Definition of nanocellulose

The term nanocellulose is often used to refer to nanoscale cellulosic material, which is considered to be in the nanoscale range if the fibril particle width is less than 100 nm. However, this term has been inconsistently used by most scholars and researchers that refer to it as microfibrillated cellulose, microfibrillar cellulose, microfibrillized cellulose, nanocellulose, nanofibrillar cellulose, nanofibrillated cellulose, and cellulose nanofibrils [1-9]. Recently, the Technical Association of the Pulp and Paper Industry (TAPPI) organization has formulated new standard terminology and definition for nanocellulose and indicated that nanocellulose can be categorized into cellulose nanofibers and cellulose nanostructured materials. Figure 4 shows the different groups of nanocellulose (TAPPI WI 3021). Cellulose nanofibers are sub-divided into nanocrystalline cellulose (or cellulose nanocrystal or cellulose nanowhisker) and NFC (or CNF). Cellulose nanostructured materials are sub-grouped into microcrystalline cellulose (or cellulose microcrystals) and microfibrillar cellulose (MFC).

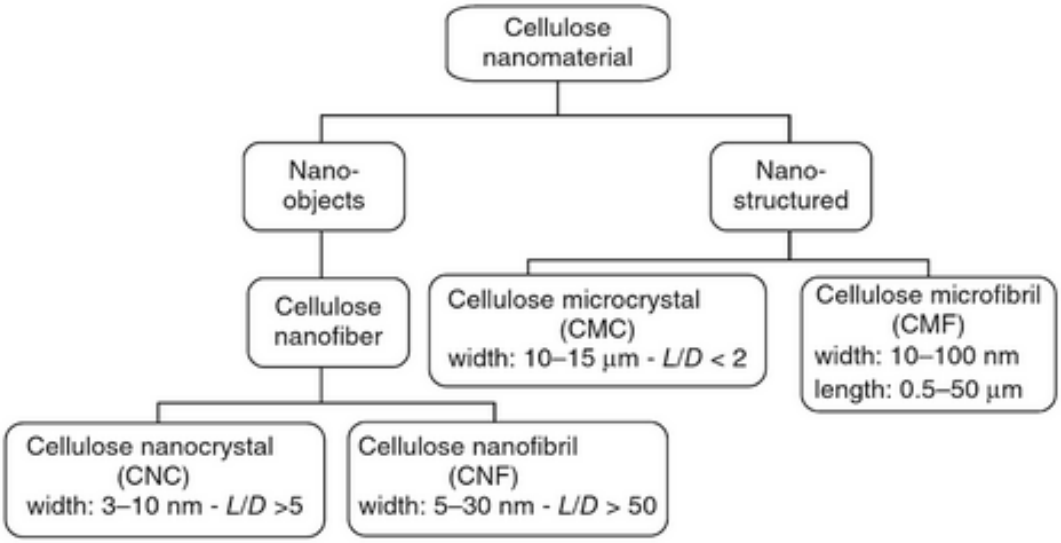

Figure 4. Standard terms for cellulose nanomaterials (TAPPI Standard WI 3021).

Cellulose crystals, cellulose microcrystal and cellulose nanocrystal (CMC and CNC), usually obtained by an acid hydrolysis are spindle-like particles showing high crystallinity and a smaller aspect ratio (length to diameter ratio) [10]. Owing to these, cellulose crystals show excellent mechanical properties that make it suitable for reinforcing materials in composite material, such as filler, plastic, and polymer [4]. In this thesis, we focus on CNF with very little attention paid to CNC.

The structure of CMF and CNF is comprised of both crystalline and amorphous regions. Typical fibril widths are 5-100 nm with a wide range of lengths, typically several micrometers by representing a higher aspect ratio than for cellulose crystals. These are pseudo-plastics similar to spaghetti-like chains and exhibiting thixotropy, the property of certain gels that show high viscous behavior in water

under normal conditions. Great disparities between NFC and MFC are found in the particle-sized distribution of cellulose nanomaterials, as has been confirmed by microscopy and image analysis [1,3,4]. CNF are usually defined as nanosized cellulosic fibrils with a diameter of less than 10nm whereas CMF has 10-100 nm of diameter. For almost 30 years, several approaches, chemical, enzymatic, or mechanical methods, have been used to extract cellulose microfibrils. However, chemical or enzymatic methods are not suitable for effective production of uniform cellulose nanofibrils because these methods are impossible to use for isolating completely individualized cellulose nanofibrils from pulp without serious damage [1]. In addition, the mechanical method for CNF is not appropriate to use due to high-energy consumption and poorly nanofibrillated cellulose [1]. Thus, some researchers have tried combining both chemical or enzymatic methods as a pretreatment and mechanical method to extract fibrils from pulp. Among them, the 2,2,6,6-tetramethylpoperidine-1-oxyl (TEMPO)-mediated oxidation method is a well-known and excellent method for obtaining well-fibrillated and individualized fibrils with high aspect ratio and a high specific surface area [1, 3]. Also, it reduces the energy consumption required for mechanical disintegration [1, 3]. That is why we chose and conducted combination TEMPO-oxidation methods and mechanical process. It is worth noting that the TAPPI and ISO naming standard proposes using cellulose nanofibrils (CNF) as standard terminology; so, in this thesis, we have decided to mostly use the term CNF.

2.2 Materials and equipment

- Bleached kraft pulps (BKPs): Commercial BKPs were used as the raw materials for the preparation of TEMPO-oxidation method. All BKPs obtained from the companies are as follow: Eucalyptus - Arauco Inc., Chile; Pine - International Paper Inc, USA; Bagasse - Resolute Forest Products, Canada. Each pulp is 100% of eucalyptus, pine, and bagasse respectively, nothing mixed with them.
- Chemicals: Sodium bromide(NaBr), TEMPO, and 10~13% sodium hypochlorite(NaClO) solution are needed for TEMPO-oxidation. These all were purchased from Sigma-Aldrich.
- High-pressure Homogenizer**:** Nano DeBEE 45-4 (BEE International Inc., USA) was employed to convert TEMPO-oxidized fibers (TOF) into CNF.

2.3 TEMPO-mediated oxidation treatment

TEMPO, which is a red-orange, sublimable solid with a melting point of 36-38°C is water-soluble, commercially available and gas stable nitroxyl radicals (Figure 5). Catalytic oxidation using TEMPO has opened a new field of efficient and selective conversion chemistry of alcoholic hydroxyl groups to aldehydes, ketones and carboxyl groups under mild conditions. In this system, catalytic amounts of TEMPO and NaBr were dissolved in polysaccharide solutions at pH 10-11, and oxidation was started by the addition of NaClO solution as a primary oxidant.

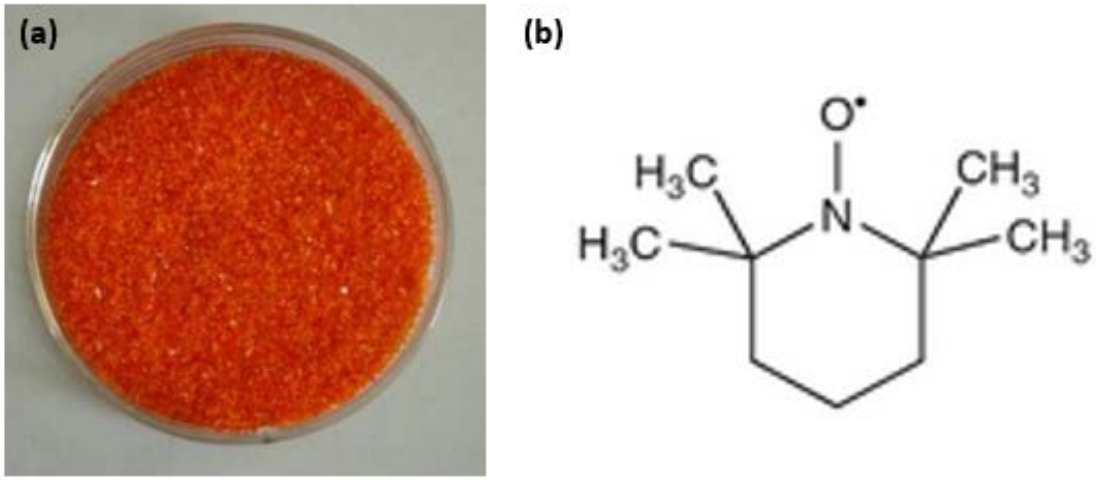

Figure 5. (a) Image of TEMPO powders and (b) representation of TEMPO chemical structure.

According to the scheme shown in Figure 6, the C6 primary hydroxyls of cellulose are expected to be oxidized to C6 carboxylate groups by TEMPO/NaBr/NaClO oxidation in water at pH 10-11 [2]. The oxidation process can be monitored from the pattern of aqueous NaOH consumption, which is continuously added to the reaction mixture to maintain the pH at 10 during the oxidation, as the C6 primary hydroxyls of celluloses can be entirely and selectively converted to C6 sodium carboxylate groups by TEMPO-mediated oxidation [2].

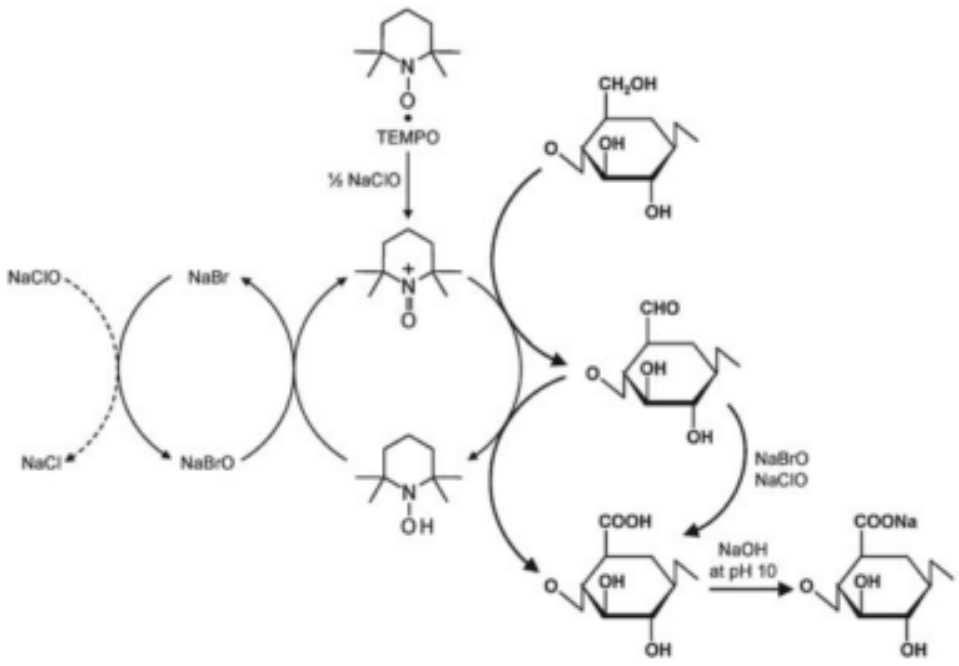

Figure 6. Schematic of TEMPO-mediated oxidation reaction with TEMPO/NaBr/NaClO.

Since the TEMPO pretreatment helped loosen the adhesion between the fibrils by preventing the formation of strong interfibrillar hydrogen bonds, the TEMPO-oxidation pretreatment of pulp is a more efficient means of extracting fibrils from most pulps [2]. The TEMPO method offers very good fibrillation efficiency with very small fiber fragments. The method is known for the high aspect ratio and large surface area of its output.

2.4 High-pressure homogenizer

The homogenization concept was introduced in the dairy and food industries, where the main aim of the technology was to stabilize food emulsions [11]. Today, the pharmaceutical, chemical, specialty food, and biotechnology industries all use high-pressure mechanical shearing equipment to emulsify, mix, disperse, and process their products [12]. Recently, the high-pressure homogenizers and microfluidizers are the most widely used equipment for extracting CNF from pulps [1, 3].

The left-hand photo of Figure 7 shows the homogenizing equipment (Nano DeBEE 45-4, BEE International Inc., USA), while the right-hand photo in Figure 7 presents a schematic of the mechanical treatment process [13]. The working principle of the high-pressure homogenizer is that it subjects the fiber suspension after TEMPO treatment to a high impact force and a high shear rate due to the reciprocating action within the valves (Figure 7) [13]. The suspension is subjected to the high-pressure treatment to reduce the fiber size so as to obtain a stable suspension. The valve seats in the homogenizer experience an increase in temperature over time during operation, but the homogenizer continues to function well even at elevated temperatures of up to 140°C. The machine can provide pressure from 15,000 psi to 35,000 psi. To get the best fibrillation of the product, we usually set pressure as 35,000 psi. After the homogenizer process, slurry of CNF looks like hydrogel (Figure 8).

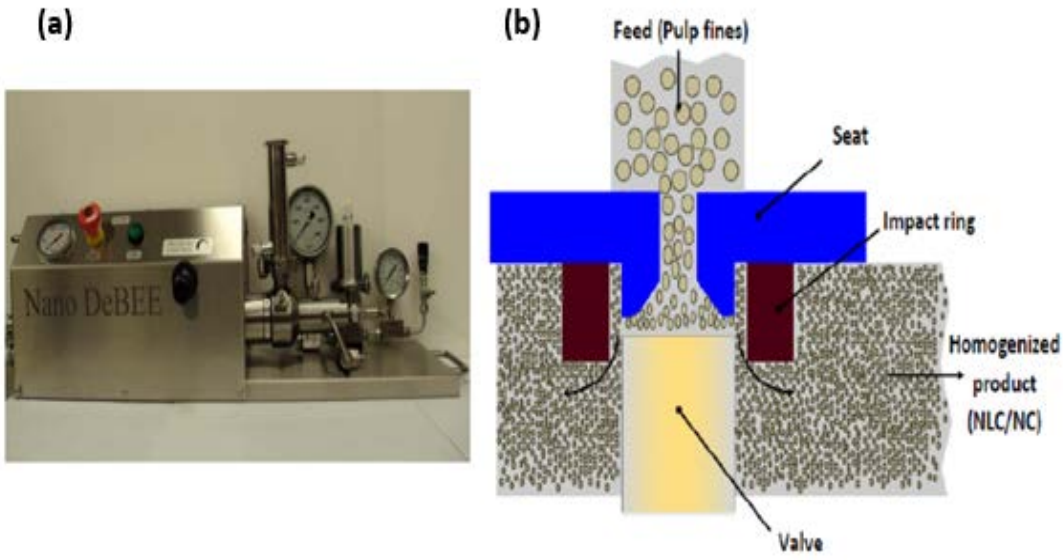

Figure 7. (a) Photo of high-pressure homogenizer and (b) a schematic of the mechanical treatment process.in the homogenizer.

Figure 8. Photos of CNF suspension after high-pressure homogenizer.

2.5 Energy consumption during nanocellulose processing

Pretreatment strategies have been developed to prevent the challenges associated with fiber clogging during homogenization and to decrease the energy consumption. Energy efficiency during nanocellulose production has been significantly improved by using pretreatment, reducing the energy consumption by over 95%, that is from 700 MJ kg^{-1} to approximately 7 MJ kg^{-1} [1]. With the same energy consumption, TEMPO-pretreated pulp fibers were more fibrillated and homogenous than were non-TEMPO pretreated fibers.

Chapter 3: Characterization of CNF and NP

3.1 Overview and background

One of objectives of the thesis is to study dimensions of CNF and physical characteristics. There are many different methods to characterize CNF. However, among them, microscopic methods, although time-consuming, are primarily used. In this thesis, we used AFM and SEM.

3.2 Microscopy techniques

3.2.1 Atomic force microscopy (AFM)

AFM is a type of scanning probe microscopy (SPM), with demonstrated resolution in nanoscale and 1000 times better than the optical microscopy. The information is gathered by interacting with the surface of a sample using a mechanical probe. Many researchers have used AFM to gain extensive information for the assessment of NFC [14]. Thus, we also used AFM to quantify and then figured out dimensions of different fibers. Due to the tendency of forming agglomeration of CNF by hydrogen bonding, we prepared a very dilute (0.001 wt%) CNF suspension to quantify a single nanofiber. The CNF suspension (10 μL) was deposited onto a freshly cleaved mica surface then air-dried. The surfaces of the specimens were scanned and imaged in tapping mode using a Dimension 5000 AFM with a Nanoscope Va controller (Veeco Instruments, USA) in air under ambient condition using tapping mode with NCHV-A standard silicon probes with aluminum reflective

coating (Bruker Inc, USA). The scan rate was set to 1 Hz and image resolution is 512 by 512 pixels. The height images and profiles were processed with WSxM 5.0.

The height images and profile of single fibers of pine are presented in Figure 9. From left to right, each image represents 1 pass, 2 passes, and 3 passes by the homogenizer. The diameter of the CNF of pine is in the range of 1 - 5 nm and its length is in the range of 200 – 800 nm shown in Figure 10. From Figure 10, we calculated the average diameter and the length of pine as follows:

- 2.1 ± 0.3 nm, 2.0 ± 1.3 nm, and 2.2 ± 1.0 nm for 1,2, and 3 passes respectively (Diameter).
- 470 ± 120 nm; 420 ± 170 nm; and 440 ± 145 nm for 1,2, and 3 passes respectively (Length).

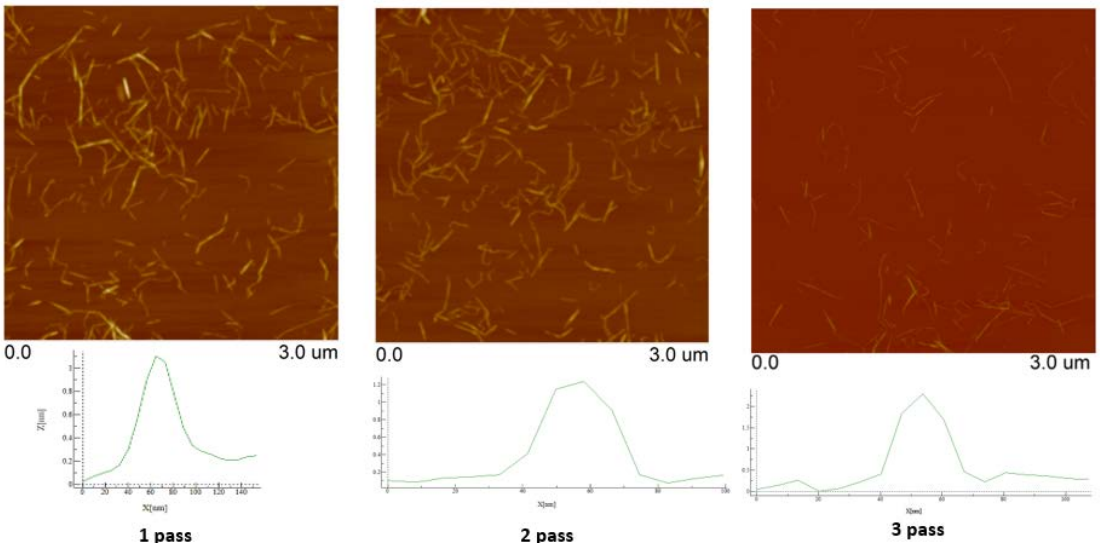

Figure 9. Height images and profiles of single fibers of pine CNF.

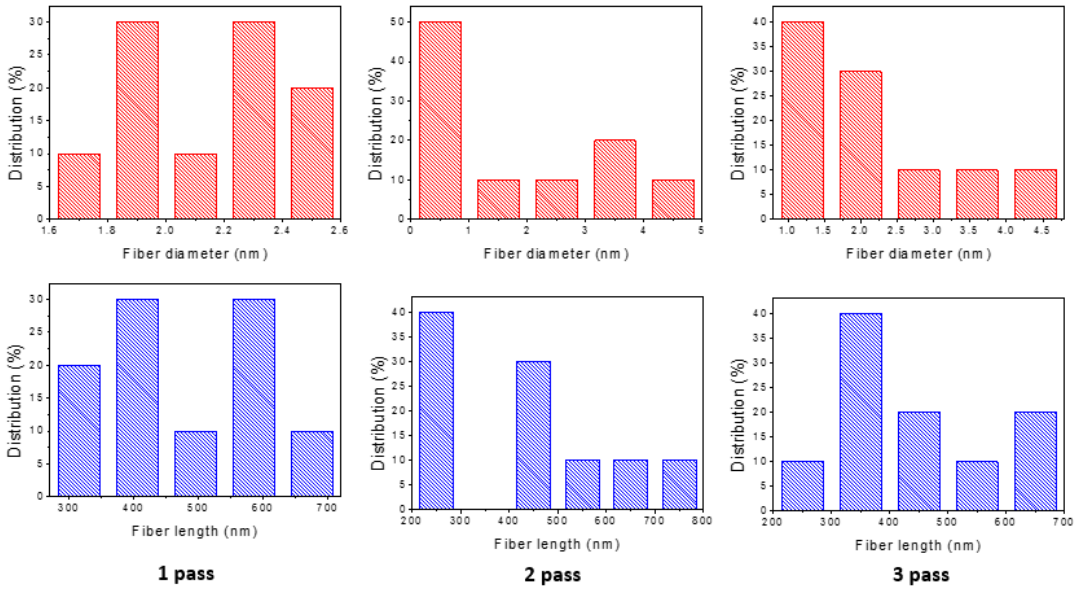

Figure 10. Histograms of pine CNF.

Figures 11 and 12 are the height image, profile and its distribution of Eucalyptus. As we did for pine, from left to right, each image represents 1 pass, 2 passes, and 3passes by the homogenizer. The height images and profile of a single fiber are presented in Figure 11. The diameter of the CNF is in the range of 1.4 - 4 nm and its length is in the range of 100 – 1200 nm shown in Figure 12. From Figure 12, we calculated average the diameter and the length of eucalyptus as follows:

- 2.2 ± 0.3 nm, 2.1 ± 0.9 nm, and 2.2 ± 0.6 nm for 1,2, and 3 passes respectively. (Diameter).
- 680 ± 160 nm; 560 ± 100 nm; and 376 ± 170 nm for 1,2, and 3 passes respectively (Length).

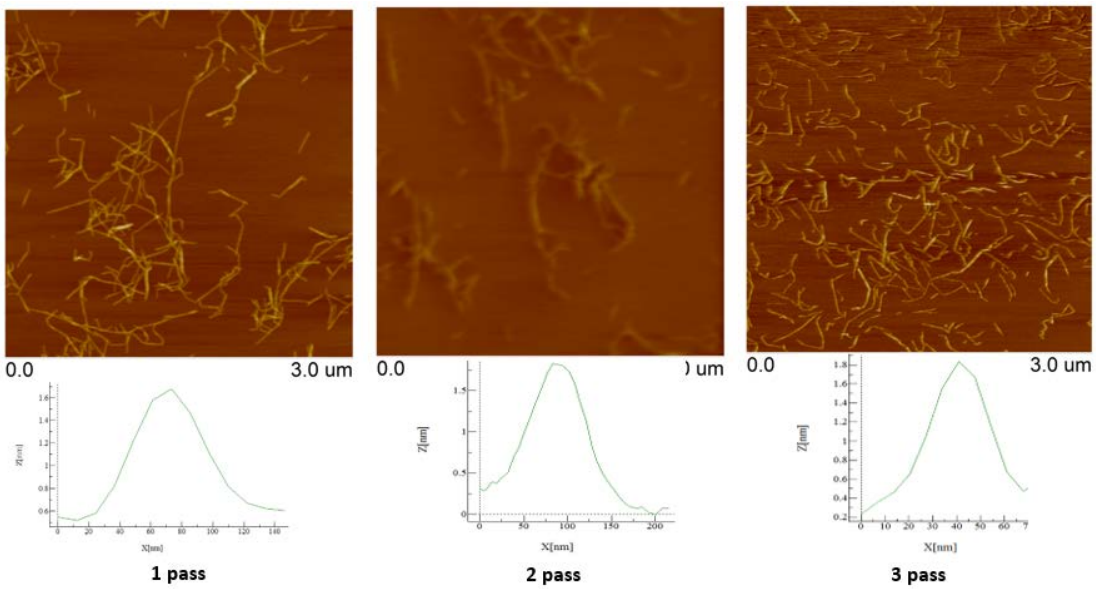

Figure 11. Height images and profiles of single fibers of eucalyptus CNF.

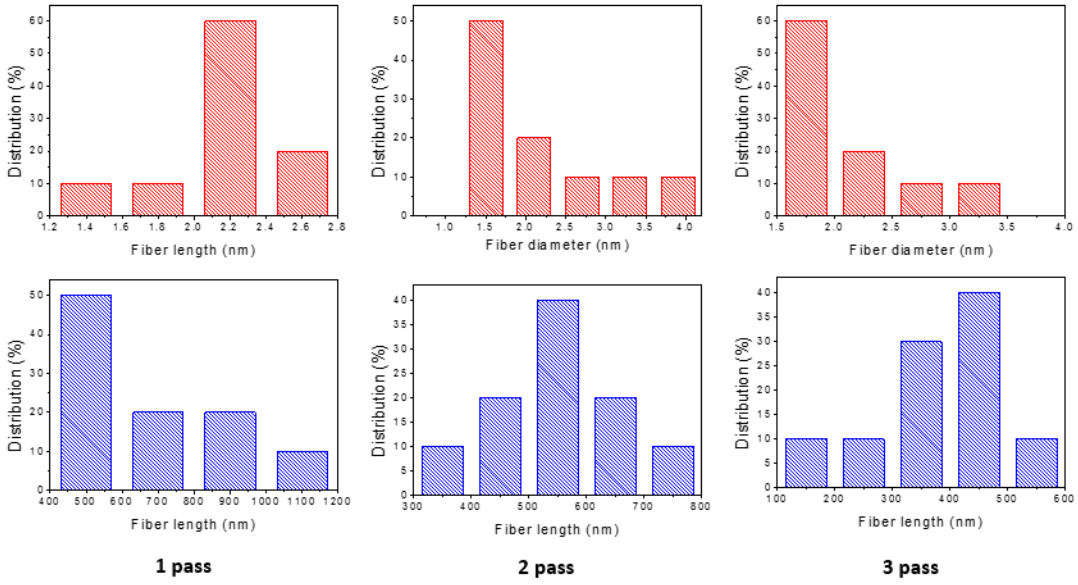

Figure 12. Histograms of eucalyptus CNF.

Figures 13 and 14 are height image, profile and its distribution of Bagasse. As we did for pine and eucalyptus, from left to right, each image represents 1 pass, 2 passes, and 3 passes by the homogenizer. The height images and profile of a single fiber are presented in Figure 13. The diameter of the CNF is in the range of 1.5 – 3.5 nm and its length is in the range of 200 – 900 nm in Figure 14. From Figure 14, we calculated average diameter and length of bagasse as follows:

- 2.1 ± 0.3 nm; 2.0 ± 0.5 nm; and 2.1 ± 0.6 nm for 1,2, and 3 passes respectively (Diameter).
- 600 ± 145 nm; 515 ± 190 nm; and 450 ± 170 nm for 1,2, and 3 passes respectively (Length).

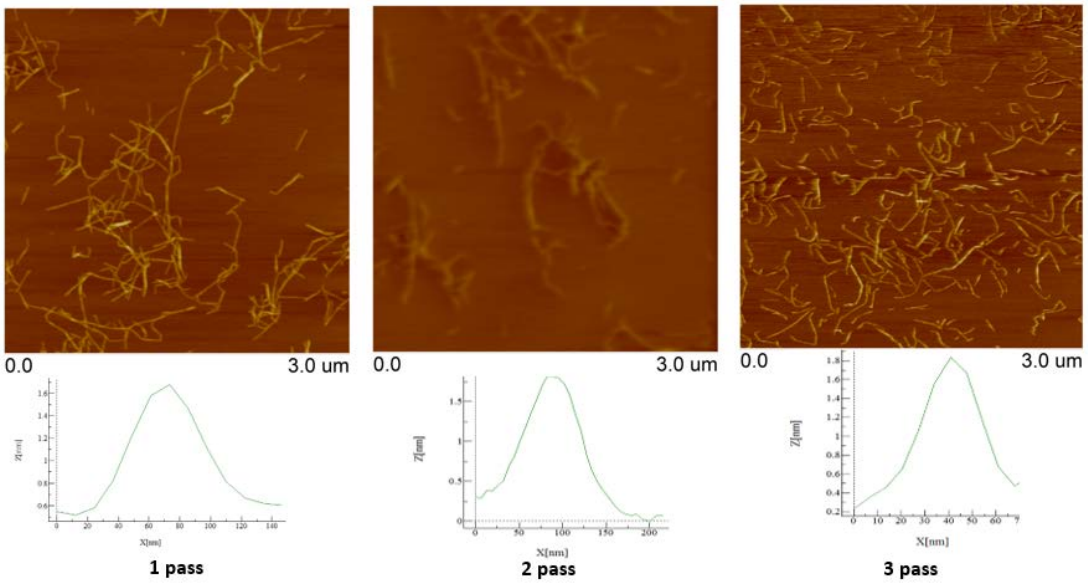

Figure 13. Height images and profiles of single fibers of bagasse CNF.

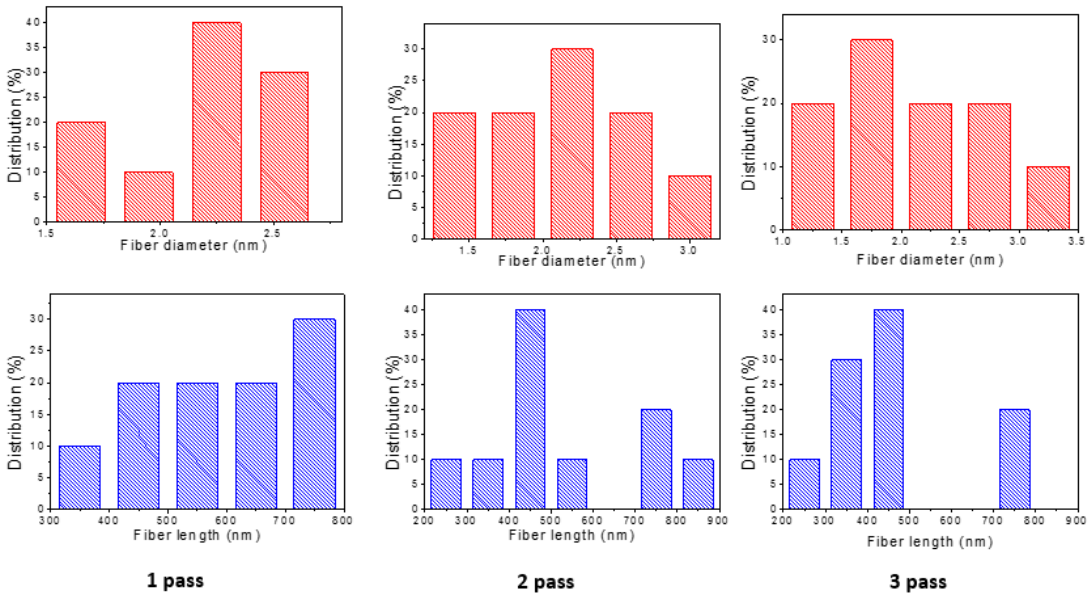

Figure 14. Histograms of bagasse CNF.

From these data, we can conclude that

- Diameters are similar among pine, eucalyptus, and bagasse (~2 nm)
- The range of nanofiber lengths based on the number of the high-pressure homogenizer passes are:
    - ~470 nm (1 pass) to ~ 440 nm (3 passes) for Pine
    - ~680 nm (1 pass) to ~ 380 nm (3 passes) for Eucalyptus
    - ~600 nm (1 pass) to ~ 450 nm (3 passes) for Bagasse
- There is aspect ratio (length / diameter) trend:

  Eucalyptus (Highest) > ***Bagasse*** > ***Pine*** (Lowest)

To check how much the high-pressure homogenizer breaks down the TOF, we got AFM images of the TOF of pine, eucalyptus, and bagasse (Figure 15). From the

data in Figure 16, we calculated average diameter and length of each TOF, shown below:

- 2.9 ± 1.3 nm for pine; 3.1± 1.4 nm for eucalyptus; and 3.1 ± 1.5 nm for bagasse (Diameter).
- 830 ± 450 nm for pine; 1027 ± 240 nm for eucalyptus; and 800 ± 310 nm for bagasse (Length).

Based on these results, TOF are thicker and longer than CNF and the high-pressure homogenizer broke the TOF down from 3 nm to 2 nm in diameter and shortened the length more than 200 nm.

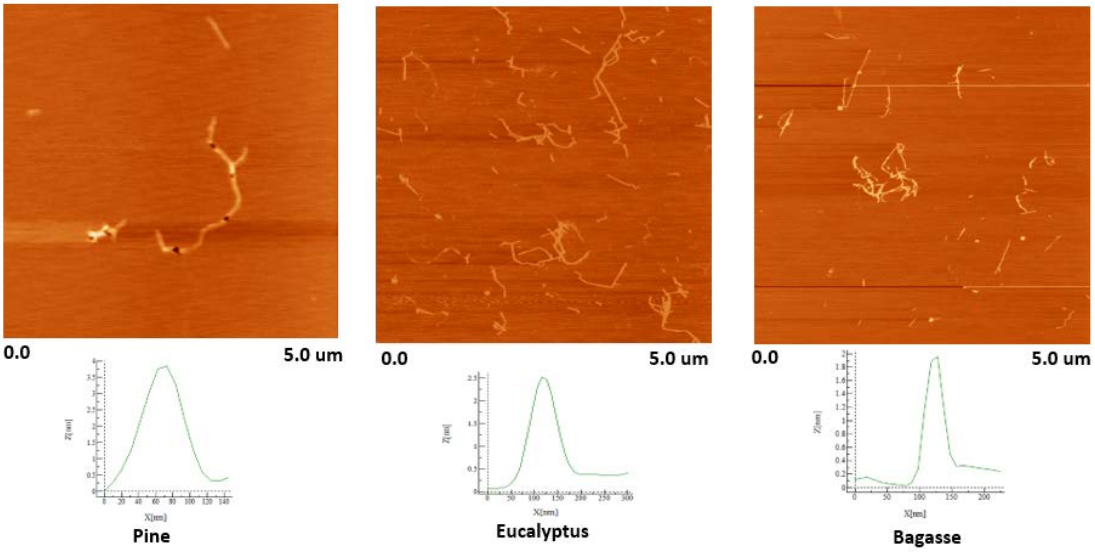

Figure 15. Height images and profiles of single fibers of pine, eucalyptus, and bagasse TOF.

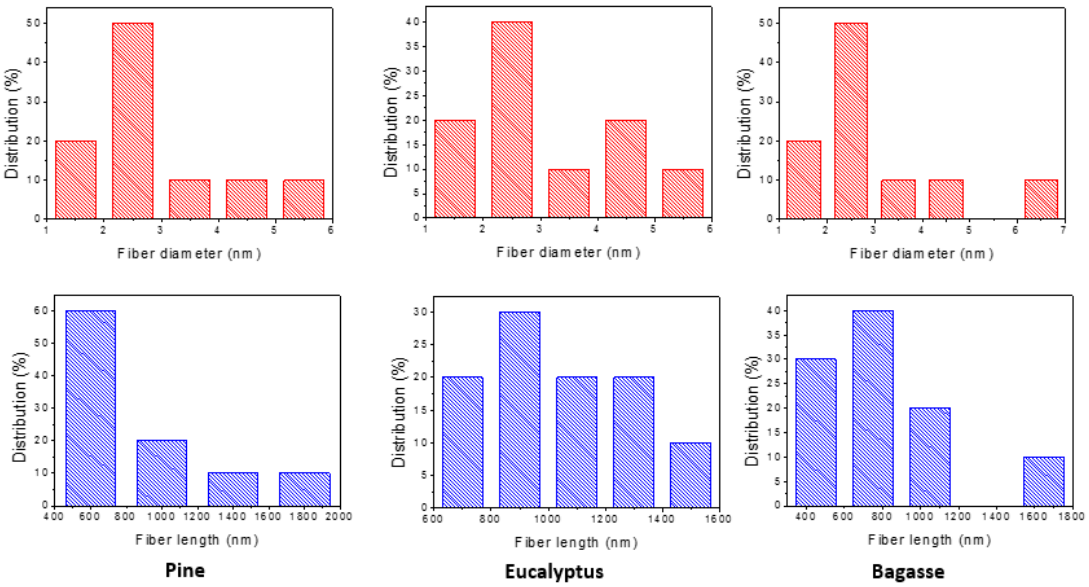

Figure 16. Histograms of pine, eucalyptus, and bagasse TOF.

We also took an AFM image of nanopaper, which has a size as 5 μm × 5 μm, and its profile data (Figure 17). This image represents that paper made by CNF has very low surface roughness. The surface root mean square (RMS) roughness was characterized on whole area and it was around 8nm which is almost same as PET as 7 nm [15].

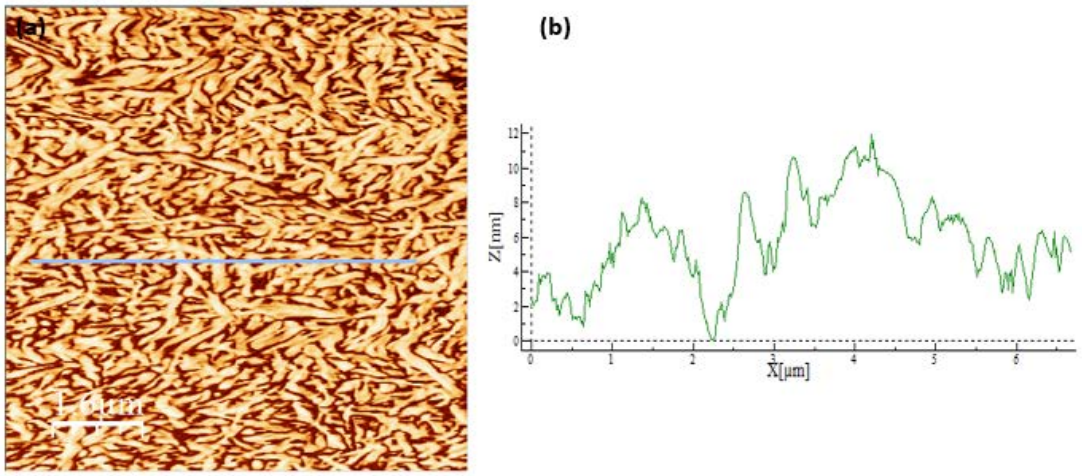

Figure 17. A height image of a nanopaper(NP) made by pine with scan size of 5 × 5 μm^2 (a) and a scanning line to show its low surface roughness (b).

3.2.2 Scanning electron microscopy (SEM)

Wood fibers are hygroscopic, radiation sensitive, and poor conductors. Therefore, it is important to prepare samples properly for SEM examination.

Researchers usually prepare the samples by freeze-drying, air-drying, or supercritical point drying. In this thesis, we chose air-drying. However, the air-drying results in some drawbacks such as drying artifacts, shrinkage, and structural collapse. To prevent these problems, we conducted the drying in a temperature-humidity chamber (LHS-150HC-II, Shanghai Bluepard Instruments Co., China) at 25 °C and 60% relative humidity. SEM images were acquired by a field emission scanning electron microscope equipped with a backscattered electron detector (FE-SEM) (SU-70 FEG SEM, Hitachi, Japan). The air-dried samples were mounted with conductive carbon tape, sputter-coated with gold for sample analysis. The working conditions

were as follows: acceleration voltage, 15 kV; pressure in the sample chamber, about 0.5 mbar; and working distance, approximately 5 mm. Figure 18 shows the surface of CNF of pine. Figure 18 (a) has the scale bar of 250 μm and (b) has smaller one which is 25 μm. The SEM images show that all CNF are randomly distributed in plane. Compared to the image of regular paper (Figure 1), paper made by CNF demonstrated a very low porous network.

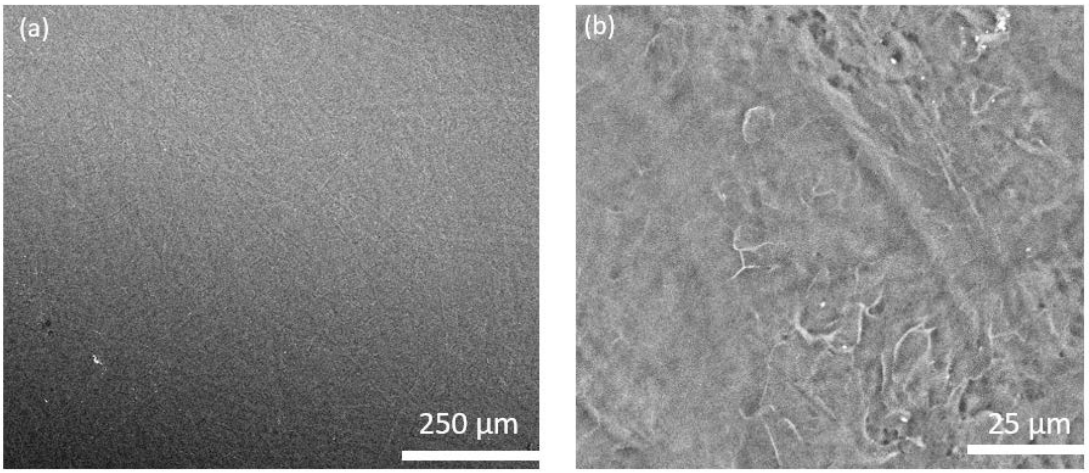

Figure 18. SEM images of NP of pine (a) and (b). (b) represents a magnified image where the scale bar is 25 μm.

3.3 Mechanical properties

The mechanical properties of substrates are significant for their applications in various areas and play an important role for the comprehensive device. The AFM and SEM images (Figures 17 and 18) show that the NFC have a random network in the plane. Films or papers (or nanopapers) made by CNF have the same network of natural cellulose fibers held together by electrostatic interactions, van der Waals

forces, and hydrogen bonds. The nanopapers which are made of CNF that are 2.2−10 nm wide and hundreds of nanometers to several micrometers in length look like a thin plastic film to the naked eye, but in fact they have a unique porous structure in the nanoscale that is totally different with traditional transparent substrates. The typical pore size is less than 100 nm (Figure 17 and 18). Due to the tightly packed nanofibrillar network (or low porosity) and numerous fiber–fiber hydrogen bonds, nanopapers possess excellent mechanical properties, such as superior tensile strength, high elastic modulus, and excellent toughness, showing their potential as a strong and lightweight substrate for green electronics or as reinforcement materials for energy application. Specifically, nanopapers with TEMPO-oxidized CNF have a higher tensile strength and higher toughness values for work-to-fracture, which are attributed to the smaller diameter of TEMPO-oxidized CNF compared to regular papers [16].

However, no one has tried and figured out the relationship between aspect ratio and mechanical properties. From the AFM data, we concluded that eucalyptus cellulosic nanofiber has a higher aspect ratio than pine. We wanted to figure out the relationship between aspect ratio and mechanical properties. In this thesis, we focused on the tensile strength and toughness. We used a Dynamic Mechanical Analysis, Q800 DMA (TA Instrument Inc., USA) under the ambient condition.

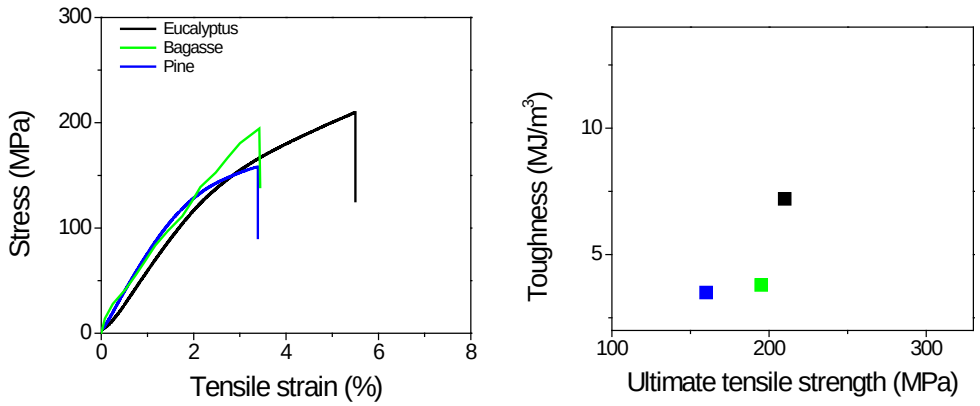

Figure 19. Stress - strain curves of cellulose paper made of pine, eucalyptus, and bagasse (left hand). Toughness - UTS curves (right hand).

Figure 19 shows stress - strain and toughness – ultimate tensile stress curves. From the figure, as the aspect ratio of cellulose fiber increases both tensile strength and toughness increase. We can conclude that higher aspect ratio nanofibers exhibit enhanced mechanical properties.

3.4 Rheological property

The suspension of CNF after exposure to the high-pressure homogenizer looks like hydrogel. To characterize the rheological property of the CNF suspension, we used an AR-2000 rheometer (TA Instrument Inc., USA) with a CC27 concentric-cylinder measuring system. The CC27 concentric cylinder has a diameter of 27 mm and a concentricity of 1 μm. The flow curves of the CNF suspensions of pine was measured. We prepared the suspension of which has 1.04 wt.% concentration. The rheological investigation was conducted at room temperature, around 25°C.

The flow curve in Figure 18 shows the rheological property of suspension in a shear rate range of 0.01–100 s^{-1}. From the flow curve presented in Figure 20, it is seen that the shear viscosity (Pa.s) of all the suspensions decrease with an increasing shear rate (s^{-1}). This suspension exhibits similar shear-thinning behavior, which reveals that they are non-Newtonian fluids.

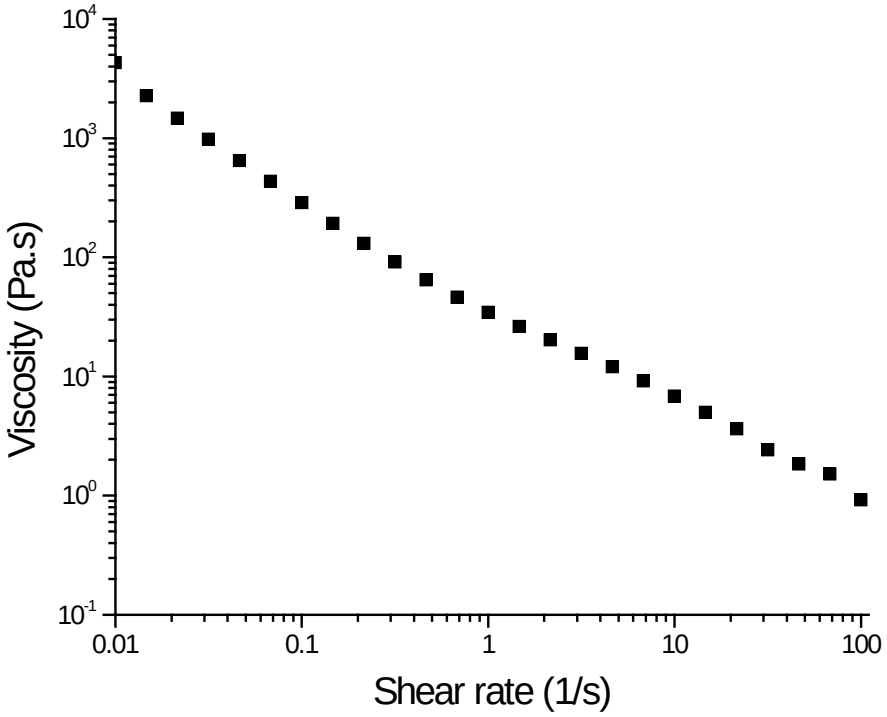

Figure 20. Rheological behavior of the suspension of CNF.

Chapter 4: Transparent films and composite films by CNF

4.1 Fabrication of a transparent film

There are several methods to fabricate a transparent film using CNF suspension, two of which are vacuum filtration and casting. Casting is superior to other methods in terms of scalability of film. Thus, we tested the casting method.

4.1.1 Film casting method

0.5 wt% of NFC suspensions after high pressure homogenizer application were prepared. 360 ml of the NFC suspension were poured into a 12 inch by 12 inch tray and allowed to dry in a temperature-humidity chamber (LHS-150HC-II, Shanghai Bluepard Instruments Co., China) by setting 25 °C and 60% relative humidity for 48 hours. The film thickness was approximately 40 ± 2 μm, and its density was 1.3 g/cm^3 (Figure 21).

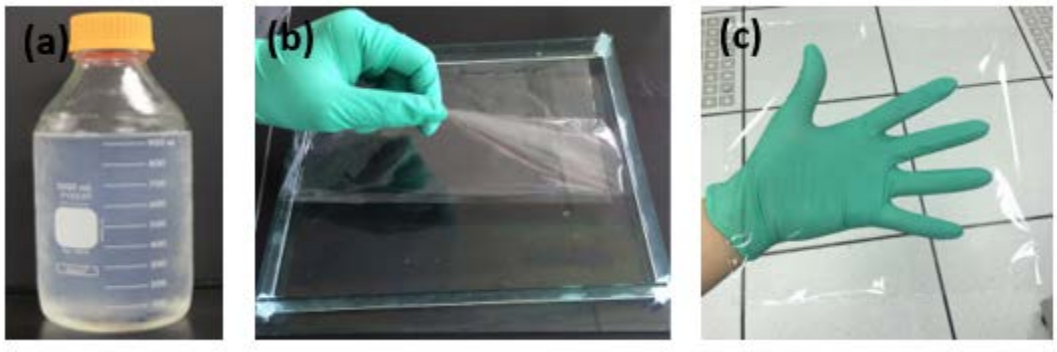

Figure 21. (a) 0.5 wt.% pine CNF (b) a transparent film detaching from the tray (c) a free-standing transparent film.

4.2 Conductive and transparent film and its properties

Since both the light transmission through the surface and electron transport along the surface is required for any optoelectronic device, introducing electrical conductivity to transparent paper is very critical. One strategy to make transparent and conductive paper is a layer-by-layer coating technique to deposit conductive materials such as CNT, graphene, and metal wires on transparent paper. These techniques include spray coating, inkjet printing, spin-coating, and Meyer-rod coating. In this research, we chose Meyer-rod coating because it is suitable for large-scaled coating. For conductive materials, we chose AgNW to minimize the loss of transmittance of the film.

4.2.1 Silver nanowire coating

Maximizing the aspect ratio and uniform networks of the AgNW promotes the highest transmittance at the lowest sheet resistance. AgNW of 50 nm diameter and 100 – 200 μm that are suspended in ethanol (purchased from ACS materials, USA) were deposited by rolling Meyer-rod with a 0.46 mm (0.018 in) wire wound rod (No. 18 wire wound rod, RD specialties, Inc.). After the coating, the sample was subjected to air-drying for 1 minute to evaporate the ethanol.

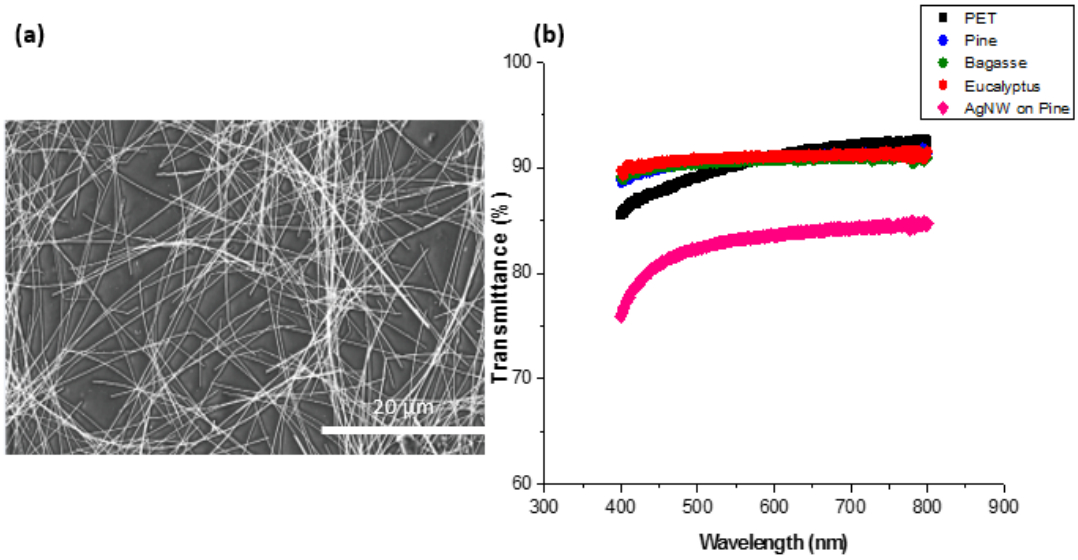

Figure 22. (a) A SEM image of AgNW on a nanopaper (b) Optical transmittance data of PET, nanopapers and nanopaper with AgNW.

Figure 22 (a) is the SEM image after Meyer-rod coating. From this, we know that AgNW were deposited on the surface of the nanopaper uniformly by forming random network. To check how much AgNW decreases the transparency of nanopaper, the optical transmittance was tested with a UV-Vis Spectromenter Lambda 35 (PerkinElmer, USA) with a Labsphere RSA-ES-20 integrating sphere between 800 and 400 nm (Figure 22 (b)). From the figure, pure nanopapers show a high transmittance of about 92% in the visible wavelength range. After coating of AgNW, the transmittance was decreased to around 82%, but it was still high enough for optoelectronic devices.

To check conductivity of the composite film, we measured sheet resistance using the 4-point probe method. The films were positioned on a stage and the four-wire measurements were recorded in ohms, with the current setting of 10 mA, and the

voltage set at 10 V. The sheet resistance of this AgNW transparent conducting paper was 20 Ω/sq.

4.3 Nanocellulose in composite film

4.3.1 Amphiphilic characteristics of cellulose

CNF suspension can disperse CNT and two-dimensional (2D) materials like graphene, molybdenum disulfide, boron nitride, etc. in water uniformly to prepare high-performance nanocomposites for advanced applications [17]. This is possible because CNF exhibit amphiphilic characteristics resulting from the presence of a hydrophobic C– H moieties and hydrophilic hydroxyl groups [17]. Figure 23 shows the chemical structure of a cellulose chain that includes hydrophilic hydroxyls and hydrophobic C–H moieties, which results in the amphiphilic character of cellulose.

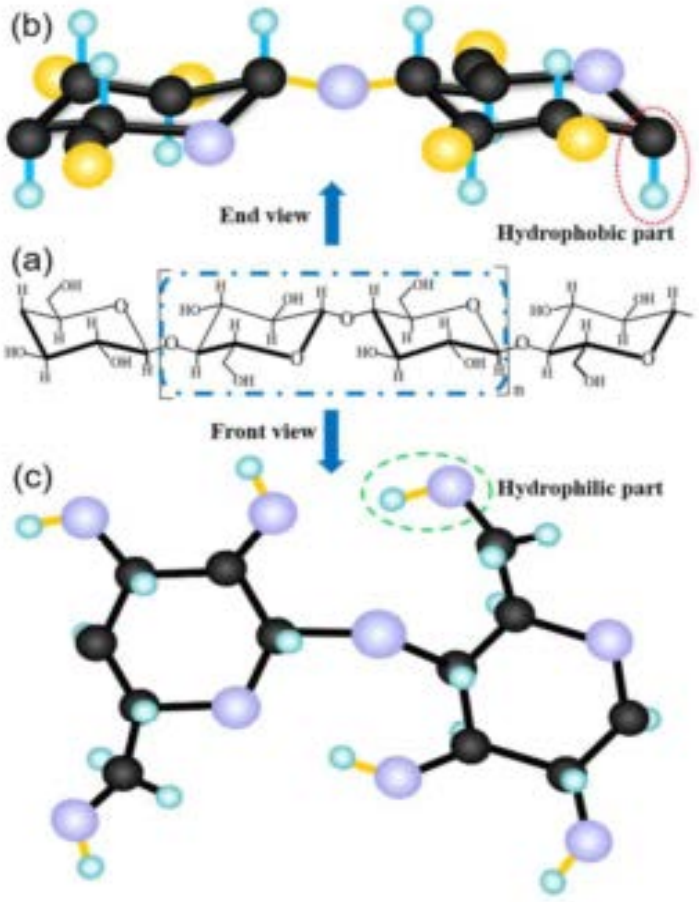

Figure 23. (a) Chemical structure of cellulose molecule. (b) End view and (c) front view of 3D a cellulose chain unit. Note that C, H, and O are shown in black, sky-blue, and indigo, respectively. The red dash circle denotes the hydrophobic C–H moiety, whereas the green dash circle represents the hydrophilic –OH moiety.

4.3.2 CNF-CNT (SWCNT) composite film

Using amphiphilic characteristics of cellulose, we tried to make a CNT suspension in water using CNF instead of surfactant. Firstly, we prepared around 1

wt.% of CNF suspension from TEMPO-oxidation and mechanical process. Single walled CNT (SWCNT) which have functional groups such as carboxyl group or hydroxyl group were purchased from Carbon Solution Inc. A total of 3 mg/mL SWCNT was added to the CNF suspension and the mixture was bath-sonicated for 5 minutes and probe sonicated with a 20% amplitude for 5 minutes to obtain a highly homogenous dispersion.

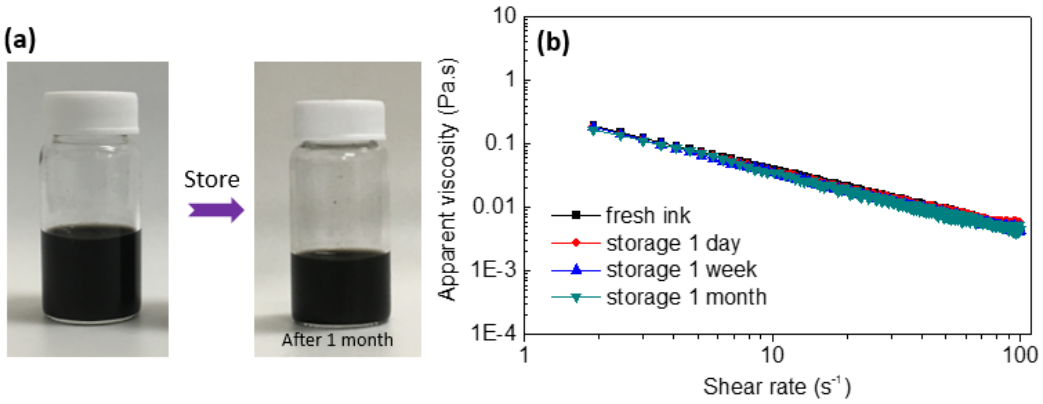

Figure 24. (a) CNF-CNT ink. Left hand one is fresh ink and right hand one is after 1 month from sonication (b) Rheological behavior of CNF-CNT ink.

After the sonication step, the CNF- SWCNT ink showed gel-like behavior and cannot see any precipitation of SWCNT after 1 month (Figure 24 (a)). This means CNF function vert well as surfactants. This fact is strongly supported by rheological behavior of CNF-CNT ink (Figure 24(b)). From the plot, there is no big difference even though we had stored this ink for a month without touching it.

To check how CNF affect mechanical properties, we used a DMA, Q800 DMA (TA Instrument Inc., USA) again to measure tensile stress and strain. We

prepared two samples: one is pure SWCNT film and the other one is CNF- SWCNT composite film. Both are prepared using the casting method in 4 cm diameter Petri dishes. Figure 25 proves that CNF make CNT paper enhance the mechanical property higher than 7 times. We speculate why adding CNF to CNT increase their mechanical property and provisionally conclude that forming strong bonding (like hydrogen bonding) between CNF and CNT improve their mechanical property.

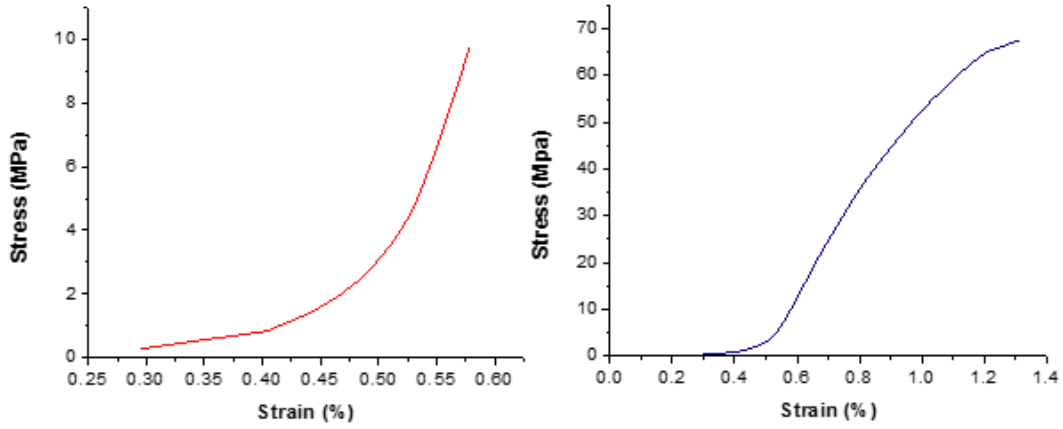

Figure 25. Stress - strain curves of pure CNT film (left) and CNF-CNT composite film (right).

Chapter 5: Conclusions

5.1 Thesis summaries and conclusions

This thesis focuses on the processing of CNF originating from bleached kraft pulp by combination of TEMPO-oxidation pretreatment and the high-pressure homogenization. In this work, we have investigated single fibers from different wood source (pine, eucalyptus, and bagasse). From our data, diameters of CNF are similar among pine, eucalyptus, and bagasse about 2nm. However, nanofiber lengths are different: 470 nm for pine, 680 nm for eucalyptus, and 600 nm for bagasse in terms of 1 pass by the high-pressure homogenizer. Also, we can see the trend that length decreases as the number of passes by the high-pressure homogenizer is increased. In addition, there is an aspect ratio (length / diameter) trend Eucalyptus (Highest) > Bagasse > Pine (Lowest). From this, we found most CNF have similar diameters but different lengths depending on type of fibers. However, because we only tested a few samples (pine, eucalyptus, and bagasse), we need to do this test with more samples from other woods or plants in the future to confirm the findings.

We have studied how the aspect ratio of CNF is related to the mechanical performance of cellulose nanopapers. Interestingly, we found a relationship which shows that tensile stress and toughness are enhanced as the aspect ratio is increased. Also, since we only tested three samples, we need more work with more samples from other woods or plants in the future to confirm the relationship between the aspect ratio and mechanical properties.

We successively produced a big size nanopaper (12 inch by 12 inch), and this shows the possibility of commercialization by using an existing traditional paper fabrication machine in industry. In addition, it shows another possibility that nanopaper can be used in optoelectronic devices owing to its high transparency and mechanical performance instead of current substrates which are made of petroleum-derived non-biodegradable materials. To overcome the weakness of nanopapers, a non-conductive material, we introduced a conductive layer using AgNW, on surface of nanopaper using the Meyer-rod coating method. AgNW were deposited on the surface and show high conductivity with sheet resistance of 20 Ω/sq without a huge decrease of transparency.

It was found that blending CNF with CNT improves the mechanical properties by forming a strong network between CNF and CNT. Tensile stress of the CNF-CNT composite film is 7 times higher than that of pure CNT film. The plausible reason for the phenomenon is hydrogen bonding between the hydroxyl groups of CNF and the carboxyl groups of CNT. We can conclude that it is also possible to produce CNF-CNT composite film with enhanced mechanical properties such being flexible, bendable, and stable. We believe that this idea would create new possibilities for technological advancement in the area of flexible substrate technology, potentially giving rise to new value-added products. However, we had not figured out that other surfactants can also influence mechanical performance and how much it improves if they do. This also could be the subject of future works.

We also checked that CNF could be used as a strength additive and a good surfactant due to the amphiphilic characteristics of cellulose. Even though it had been

stored for a month, we could not see any precipitation or big difference in rheological behavior.

Lastly, we introduced and conducted CNF processing from pulp, which is called green materials, with low energy consumption. Owing to physical properties of nanopapers compared to existing flexible substrate such as PET, CNF and their applications can be applied to a variety of materials field by solving environmental problems which result from materials derived from petroleum.

Bibliography

[1] H. Zhu, W. Luo, P. N. Ciesielski, Z. Fang, J. Y. Zhu, G. Henriksson, M. E. Himmel, and L. Hu, “Wood-Derived Materials for Green Electronics , Biological Devices , and Energy Applications,” *Chem. Rev*, *116*, 9305, 2016

[2] A. Isogai, T. Saito, and H. Fukuzumi, “TEMPO-oxidized cellulose nanofibers.,” *Nanoscale*, vol. 3, no. 1, pp. 71–85, 2011.

[3] H. Zhu, Z. Fang, C. Preston, Y. Li, and L. Hu, “Transparent paper: fabrications, properties, and device applications,” *Energy Environ. Sci.*, vol. 7, no. 1, pp. 269–287, 2014.

[4] Z. Fang, H. Zhu, W. Bao, C. Preston, Z. Liu, and J. Dai, “Environmental Science Highly transparent paper with tunable haze for green electronics,” *Energy Environ. Sci.*, vol. 7, pp. 3313–3319, 2014.

[5] T. Taipale, M. Österberg, , A. Nykänen, J. Ruokolainen, and J. Laine, “Effect of microfibrillated cellulose and fines on the drainage of kraft pulp suspension and paper strength,” *Cellulose* 17: pp1005–1020, 2010

[6] Ø. Eriksen, K. Syverud, Ø. Gregersen, “The use of microfibrillated cellulose produced from kraft pulp as strength enhancer in TMP paper,” *Nordic Pulp and Paper Research Journal*., 23(3), 299–304, 2008

[7] H. Zhu, L. Hu, J. Cumings, J. Huang, and Y. Chen, “Highly Transparent and Flexible Nanopaper Transistor.,” *ACS Nano*, no. 3, pp. 2106–2113, 2013.

[8] K. Syverud, G. Chinga-Carrasco, J. Toledo, and P. G. Toledo, “A comparative study of Eucalyptus and Pinus radiata pulp fibres as raw materials for production of cellulose nanofibrils,” *Carbohydr. Polym.*, vol. 84, no. 3, pp. 1033–1038, 2011.

[9] M. Hassan, A. Mathew, E Hassan, and K.Oksman, “Effect of pretreatment of bagasse pulp on properties of isolated nanofibers and nanopaper sheets,” *Wood and Fiber Science*, 42, 362–376, 2010.

[10] M. Mariano, N. El Kissi, and A. Dufresne, “Cellulose nanocrystals and related nanocomposites: Review of some properties and challenges,” *J. Polym. Sci. Part B Polym. Phys.*, vol. 52, no. 12, pp. 791–806, 2014.

[11] P. Paquin, “Technological properties of high pressure homogenisers: the effect of fat globules, milk proteins, and polysaccharides,” *International Dairy Journal* 9, 329–335

[12] P. Floury, A. Desrumaux, and J. Lardieres, “Effect of high-pressure homogenisation on droplet size distribution and rheological properties of model oil-in-water emulsions,” *Innovative Food Science and Emerging Technologies* 1, 127–134. 2000

[13] Osong, S.H. (2016), “*Mechanical Pulp-Based Nanocellulose* (Doctoral thesis),” Retrieved from DiVA-portal.org (ISBN 978-91-88025-64-7)

[14] I. Usov, G. Nyström, J. Adamcik, S. Handschin, C. Schütz, A. Fall, L. Bergström, and R. Mezzenga, “Understanding nanocellulose chirality and structure-properties relationship at the single fibril level.,” *Nat. Commun.*, vol. 6, no. May, p. 7564, 2015.

[15] H. Zhu, Z. Xiao, D. Liu, Y. Li, N. J. Weadock, Z. Fang, J. Huang, L. Hu, “Biodegradable transparent substrates for flexible organic-light-emitting diodes,” *Energy Environ. Sci.* **2013**, *6*, 2105.

[16] H. Zhu, S. Zhu, Z. Jia, S. Parvinian, Y. Li, O. Vaaland, L. Hu, and T. Li, "Anomalous scaling law of strength and toughness of cellulose nanopaper," *Proc. Natl. Acad. Sci.*, no. February 2016, pp. 1–6, 2015.

[17] S Ming, C. Gang, Z. Wu, L. Su, J. He, Y. Kuang, and Z. Fang, "Effective dispersion of aqueous clay suspension using carboxylated nanofibrillated cellulose as dispersant," *RSC Adv.*, 2016.